BACHMANN, R., KREUER, K. D., RABENAU, A. & SCHULZ, H. (1982). *Acta Cryst.* B**38**, 2361–2364.
BACHMANN, R. & SCHULZ, H. (1983). *Solid State Ionics*, **9–10**, 521–524.
BECKER, P. J. & COPPENS, P. (1974). *Acta Cryst.* A**30**, 129–147.
DENES, G., PANNETIER, J., LUCAS, J. & LE MAROUILLE, J. Y. (1979). *J. Solid State Chem.* **30**, 335–343.
International Tables for X-ray Crystallography (1974). Vol. IV. Birmingham: Kynoch Press. (Present distributor D. Reidel, Dordrecht.)
KOHLER, H., SCHULZ, H. & MELNIKOV, O. (1983). *Mater. Res. Bull.* **18**, 1143–1152.
SCHULZ, H. & ZUCKER, U. H. (1981). *Solid State Ionics*, **5**, 41–46.
VILMINOT, S., BACHMANN, R. & SCHULZ, H. (1983). *Solid State Ionics*, **9–10**, 559–562.
WILLIS, B. T. M. (1969). *Acta Cryst.* A**25**, 277–300.
ZUCKER, U. H., PERENTHALER, E., KUHS, W. F., BACHMANN, R. & SCHULZ, H. (1983). *J. Appl. Cryst.* **16**, 358.
ZUCKER, U. H. & SCHULZ, H. (1982*a*). *Acta Cryst.* A**38**, 563–568.
ZUCKER, U. H. & SCHULZ, H. (1982*b*). *Acta Cryst.* A**38**, 568–576.

Acta Cryst. (1988). B**44**, 236–242

Oriented Intergrowth of an Antigorite and an Arsenate Mineral from Långban, Sweden. A Natural Composite Material

BY STAFFAN HANSEN* AND MICHAEL O'KEEFFE

Department of Chemistry, Arizona State University, Tempe, AZ 85287, *USA*

(*Received* 24 *September* 1987; *accepted* 4 *January* 1988)

Abstract

'Asbestos–hedyphane' is a well oriented intergrowth of antigorite and a Pb,Ca arsenate of apatite type from Långban, Sweden. The outer appearance is strikingly similar to that of a yellowish chrysotile–asbestos. Examination by scanning electron microscopy and energy dispersive analysis of emitted X-ray radiation reveals flexible antigorite laths of nearly ideal serpentine composition, $Mg_3Si_2O_5(OH)_4$, intergrown with a chloride-poor hedyphane-like mineral (hedyphane is $Pb_3Ca_2As_3O_{12}Cl$). Hexagonal unit cell of the arsenate, as determined by powder X-ray diffraction: $a =$ 10·0547(8), $c = 7{\cdot}310(2)$ Å. Four fibers were examined by Weissenberg and oscillation techniques. The antigorite exhibits a monoclinic lattice with $a = m \times 2{\cdot}5$, $b = 9{\cdot}2$, $c = 7{\cdot}3$ Å, $\beta = 91{\cdot}5°$ (m integer). Electron diffraction patterns from nine antigorite laths showed that m is variable, with $14 \le m \le 20$. Texture of the intergrowth as determined from X-ray diffractographs: **c**(arsenate) ∥ **b**(antigorite) ∥ fiber axis; extensive rotational disorder around the fiber axis, though a preferred orientation is observed after every 60° of rotation. This is probably due to a lattice fit: (001)antigorite ∥ $(10\bar{1}0)$arsenate, $4a$(antigorite) ≃ a(arsenate) and $4b$(antigorite) ≃ $5c$(arsenate) if $m = 1$. A second preferred orientation, observed in the middle of the 60° intervals, may be due to a lattice fit: (001)antigorite ∥ $(11\bar{2}0)$arsenate, $7a$(antigorite) ≃ $3^{1/2}a$(arsenate), $4b$(antigorite) ≃ $5c$(arsenate).

Introduction

The mineral aggregate 'asbestos–hedyphane' from Långban, Sweden, was characterized by Sjögren (1891, 1892) as follows: 'The designation of a peculiar compound of two minerals, found at Långban for some years in different parts of the mine. It formed fibrous aggregates up to an inch in length of a grey to brownish colour and silky lustre. A microscopical examination has shown that it is composed of two different minerals of which one, in the form of thin needles with a starlike intersection permeates the other, and gives the whole compound a fibrous asbestos-like appearance. The needle-like mineral is a hydrous silicate of magnesia with a composition similar to that of serpentine; the other mineral is chiefly an arseniate of lead with some lead chloride, but it does not seem to be identical with the common hedyphane.' The chemical data were later published by Magnusson (1930, pp. 53–54). Dunn, Rouse & Nelen (1985) have described a fibrous hydroxyl-bearing hedyphane from Långban, but no silicate phase was characterized.

The present study was undertaken to elucidate further the nature of 'asbestos–hedyphane'. Since the cell parameters of serpentine minerals and hedyphane both exhibit a 7·3 Å repeat, the possibility of an epitaxial relationship between the two phases was indicated. An epitaxial relation was indeed found, but the 7·3 Å axes are perpendicular.

After the completion of this work, a study of a similar material (Kautz, 1967) has come to our attention. Kautz describes a crystallographically well ordered intergrowth of hedyphane and antigorite. The main conclusions of Kautz are confirmed in the present

* Present address: National Center for HREM, Inorganic Chemistry 2, Chemical Center, University of Lund, PO Box 124, S-221 00 Lund, Sweden.

0108-7681/88/030236-07$03.00

study and extended data are presented concerning the texture of intergrowth and the modulation wavelength of antigorite.

Scanning electron microscopy

Two specimens collected in the summer of 1975, on the mine dumps in Långban, were used in this study. The first specimen consists of dolomite and fine-grained jacobsite, and the 'asbestos–hedyphane' occurs as up to 5 mm long fibers of a pale yellowish-white color, associated with 1 cm hematite crystals and some calcite. The other specimen contains dolomite and calcite with cm large areas of a mixture of a white massive arsenate and fibrous 'asbestos–hedyphane'.

Fibrous material was removed from the specimens and fibers were then mounted on a holder with conducting glue. A thin layer of gold was evaporated onto the samples which were then studied in a JSM-T200 scanning electron microscope. The micrographs reveal an intimate intergrowth of long laths and a massive material, see Fig. 1. These laths have a width in the order of 10 μm, while the thickness is a fraction of a micrometer. Since the length of these laths is measured in centimeters, their habit can be classified as truly asbestiform. Some mechanical damage, induced when the fibers were broken loose from the matrix, is also evident in the pictures. The massive material has sometimes been separated from the laths. The laths are flexible, compared to the massive material, which is brittle and cracks into pieces. It can be seen that the laths form at least three sets of angles (60, 90 and 120°) when they intersect.

A chemical analysis of a crushed sample of 'asbestos–hedyphane' was performed by H. van Ass, at Philips in Eindhoven, The Netherlands. It proved possible to analyze the two components separately in a Philips SEM 515 scanning microscope, equipped with an EDAX 9100 system for energy dispersive analysis of characteristic X-ray radiation, emitted after excitation with 15 or 30 kV electrons. For Al, Si, Mg, Mn and Fe the *K* peaks were measured, for As and Ba the *L* peaks, and for Pb the *M* peak. The data were ZAF corrected and no standards were used. With pentavalent As and divalent Pb the resulting composition of the arsenate is $(Pb_{3\cdot44}Ca_{1\cdot02}Ba_{0\cdot12})_{\Sigma 4\cdot58}As_{3\cdot17}O_{12\cdot5}$. This can be compared to the ideal formula of a hypothetical hydroxyl hedyphane: $Pb_3Ca_2As_3O_{12}(OH)$ or $Pb_3Ca_2As_3O_{12\cdot5}\cdot\frac{1}{2}H_2O$. The 'anhydrous' composition of the laths is $(Mg_{2\cdot93}Fe_{0\cdot05}Al_{0\cdot03}Mn_{0\cdot01})_{\Sigma 3\cdot02}(Si_{1\cdot95}Al_{0\cdot03})_{\Sigma 1\cdot98}O_7$ if all cations except Si^{4+} and Al^{3+} are assumed to be divalent and Al is split equally between the octahedral and the tetrahedral sites. The ideal serpentine formula can be written as $Mg_3Si_2O_7.2H_2O$.

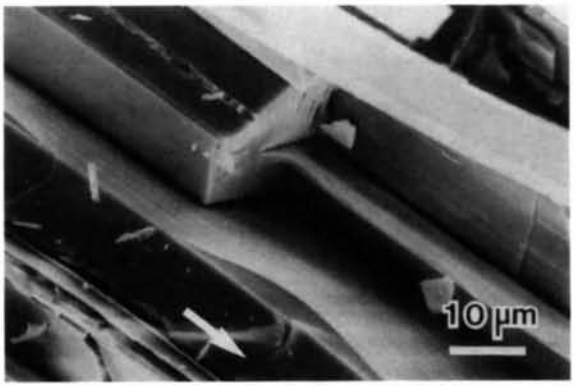

Fig. 1. Scanning electron micrograph of the oriented intergrowth consisting of flexible silicate laths in a massive and brittle arsenate. The arrow indicates the direction of **b** (antigorite) and **c** (arsenate).

X-ray diffraction

Guinier–Hägg powder photographs, recorded with Cu $K\alpha_1$ radiation, show no lines which must be referred to the silicate phase, *i.e.* all lines are indexable on the basis of the hexagonal unit cell of the arsenate. Powder diffraction patterns of the fibrous and the massive materials, found in one of the specimens, are identical. A least-squares refinement using the glancing angles of 40 single indexed powder lines gave the following cell parameters for the arsenate: $a = 10{\cdot}0547\ (8)$, $c = 7{\cdot}310\ (2)$ Å. This is similar to what Kautz (1967) and Dunn, Rouse & Nelen (1985) report. The silicate is shown below to be an antigorite, a monoclinic serpentine mineral with a supercell given by Bailey (1984) as $a = m \times 2{\cdot}55$, $b = 9{\cdot}23$, $c = 7{\cdot}27$ Å, $\beta = 91{\cdot}6°$ (m is an integer).

Four fibers in all were mounted on glass needles, and a Nonius Weissenberg camera using Cu $K\alpha$ radiation was utilized to obtain X-ray diffraction patterns with the fiber axis aligned along the axis of the camera. The fibers were about 1 mm long and a few tenths of a mm in diameter. Two of the fibrous aggregates produced reflections exclusively from a hedyphane-like phase with a rotation axis of 7·3 Å. The other two were diphasic, since two sets of layer lines could be identified in the oscillation photographs.

Some diffraction patterns from the first of the diphasic samples are presented in Fig. 2. The layer lines corresponding to a rotation axis of 7·3 Å contain distinct reflections, while the second set of layer lines gives a rotation axis of 9·2 Å and exhibits strong streaking between the reflections on a line, see Fig. 2(*a*). For the 9·2 Å silicate phase, the intensity of every third layer line is much higher than the rest. All layer lines are parallel and the reflections show no arcing, even at high scattering angles. This indicates a very well oriented intergrowth with parallel axes (Wicks & Zussman, 1975). Some 'oscillation' photographs were recorded with the crystal fixed, *i.e.* without rotation, see

Fig. 2(*b*). The silicate layer lines are not affected when the oscillation is stopped, while the arsenate reflections are reduced in number. This implies that the silicate crystals are subject to extensive rotational disorder, in contrast to the more single-crystal-like behavior of the arsenate, *i.e.* only a few reflections fulfill the requirements of Bragg's law for a fixed angle of rotation.

The same thing is evident in the corresponding zero-level Weissenberg zone, Fig. 2(*c*), where the silicate and arsenate patterns are superimposed. The arsenate shows a spot pattern with reflections elongated in the horizontal direction, indicating some rotational disorder for this phase also. The silicate reflections, on the other hand, have degenerated into almost continuous horizontal streaks. An *a*-axis repeat of 10·1 Å was determined for the arsenate, by measurement of some *hh*0 and *h*00 reflections. The three horizontal silicate lines of lowest scattering angle gave spacings of 7·28, 3·65, 2·56 Å, respectively. Closely spaced silicate lines indicate a long-period structure. An inspection of the intensity distribution along the strongest lines reveals features of high intensity which are repeated at 60° intervals. Thus the rotational disorder of the silicate laths is extensive, but they are not completely randomly oriented.

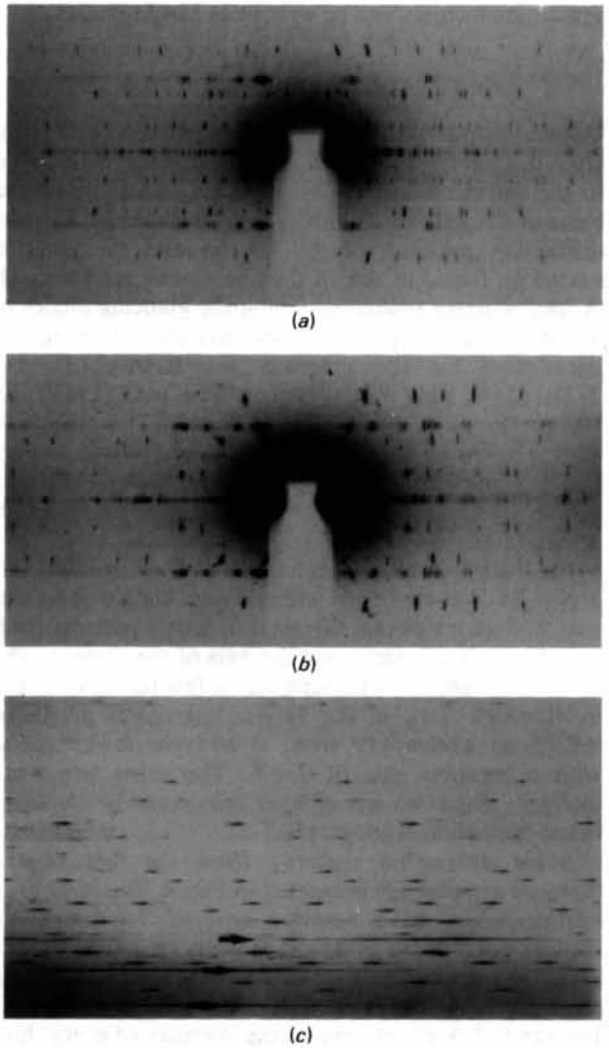

Fig. 2. X-ray diffractographs of a fiber aggregate. (*a*) Oscillation ±15°. Layer lines from antigorite are streaked, while layer lines from the arsenate show sharp reflections. (*b*) Fiber in fixed position. The number of arsenate reflections is reduced. (*c*) Zero-level Weissenberg zone: *h*0*l* antigorite and *hk*0 arsenate. Arsenate spots are elongated, while antigorite gives horizontal streaks (three low-angle antigorite lines are marked by arrows).

In the second sample, which contained both arsenate and silicate, no reduction in the number of arsenate reflections could be observed when diffractographs taken with and without oscillation were compared. The higher degree of rotational disorder for the arsenate crystals was also confirmed by more extensive streaking in the zero-order Weissenberg pattern. The lowest Weissenberg zones in which the silicate and the arsenate layer lines could be completely separated, by carefully trimming the screen slit position, were *hk*2 (arsenate) and *h*3*l* (silicate). In Fig. 3, an *h*3*l* zone of the silicate is presented. As before, a set of closely spaced horizontal lines are prominent in the photograph. Small line separations are due to the superlattice along **a** in antigorite. The continuous horizontal lines are generated by extensive rotational disorder (∥ to **b**) among the antigorite crystals. Maxima of intensity occur as before after every 60° of rotation. But here weaker maxima can also be seen in the center between two maxima separated by 60°. This suggests the presence of two preferred orientations. Another feature of interest is the continuous reciprocal curves which are repeated with 60° separations. These stem from streaks along $\mathbf{c}^*$ caused by stacking disorder in antigorite. A set of reflection pairs caused by twinning on {001} are indicated in Fig. 3. A horizontal splitting of 3° can be measured and this can be compared to the ideal value of $2 \times 91{\cdot}6° - 180° = 3{\cdot}2°$ (Bailey, 1984).

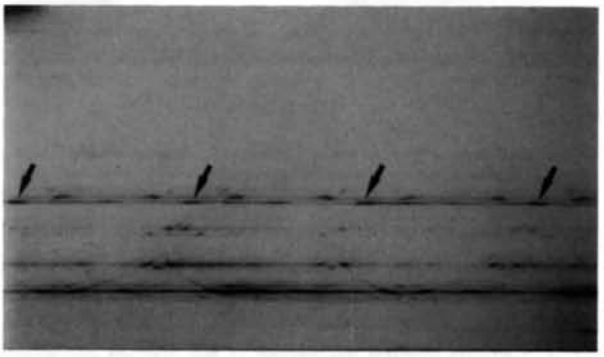

Fig. 3. Weissenberg: *h*3*l* zone of antigorite in another arsenate–silicate fiber. Pairs of reflections indicative of twinning are indicated by arrows at 60° intervals.

Transmission electron microscopy

In order to characterize the silicate laths further, the material was investigated in a JEM-200CX transmission electron microscope, operated at 200 kV. A few fibers were crushed with methanol in an agate mortar and this dispersion was then used to deposit some of the material on a copper grid covered by a holey carbon film. Diffraction patterns were recorded at a camera length of 77 cm.

Approximately equal-sided grains were identified by their diffraction patterns as being the arsenate phase. The laths were easily recognized by their habit and their transparency in the electron beam at medium magnifications, see Fig. 4. Owing to the habit of the crystals, all diffraction patterns show the same orientation, *i.e.* the a^*b^* plane of antigorite. In order to determine the variable a repeat, the reciprocal lattices were carefully measured and the ratio a/b was determined. This ratio was then compared to theoretical values calculated as $(m \times 2{\cdot}55)/9{\cdot}23$. Superlattice spacings ranging from $m = 14$ to $m = 20$ were found when nine crystals were investigated. Most laths only give one specific value of m, but the crystal shown in Fig. 4 exhibits $m = 15$ in the upper part of the crystal and $m = 16$ in the lower part.

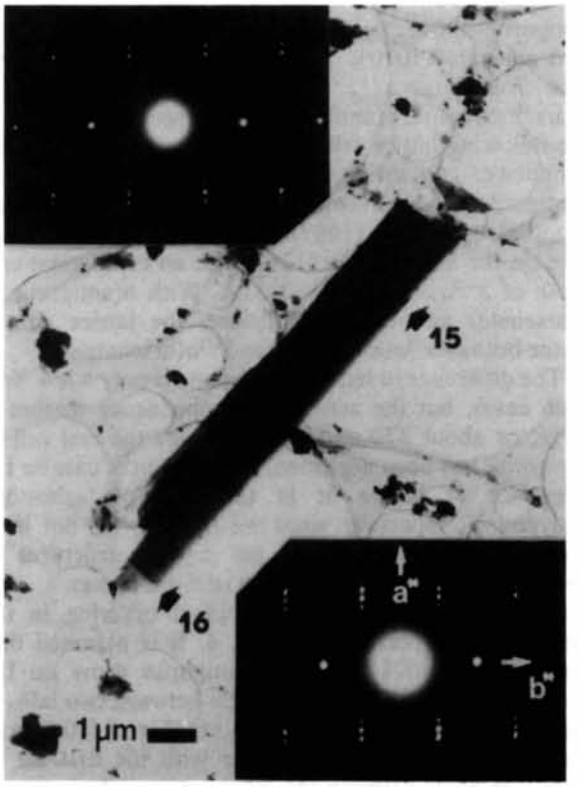

Fig. 4. Transmission electron micrograph of an antigorite lath exhibiting different superlattices along **a** in the two areas marked by arrows ($a = m \times 2{\cdot}55$ Å). The corresponding a^*b^* electron diffraction patterns with $m = 15$ and 16 are included.

A careful inspection of the corresponding diffraction patterns reveals streaking along **a***, which indicates the presence of several lattice repeats within the diffracting area.

Discussion

Arsenate

The mineral hedyphane was recently redefined (Rouse, Dunn & Peacor, 1984), as the ordered intermediate phase $Pb_3Ca_2As_3O_{12}Cl$ (apatite structure), which occurs in the system $Pb_5As_3O_{12}Cl$ (mimetite)–$Ca_5As_3O_{12}Cl$ (turneaureite; Dunn, Petersen & Peacor, 1985).

The formula of the arsenate reported by Magnusson (1930) becomes $(Pb_{2{\cdot}58}Ba_{0{\cdot}18})_{\Sigma 2{\cdot}76}(Ca_{1{\cdot}46}Mn_{0{\cdot}29}Fe_{0{\cdot}04})_{\Sigma 1{\cdot}79}(As_{2{\cdot}85}P_{0{\cdot}13})_{\Sigma 2{\cdot}98}O_{12}Cl_{0{\cdot}47}$, after deduction of MgO. Chemical analysis of the arsenate in our specimens suggests the presence of a member which is poor in chlorine, but the OH/F contents have not been determined, so no further conclusions can be drawn. The mineral shows an excess of lead over the ideal 3:2 ratio although this is not a problem, since Rouse *et al.* (1984) found a gap on the Ca-rich side of the system and a continuous series on the Pb-rich side.

The arsenate crystals in our sample are needle-like, with c as the axis of elongation. This is a somewhat unusual habit, since hedyphane crystals are commonly flattened on {0001} (Rouse *et al.*, 1984) or pyramidal (Sjögren, 1892; Palache & Berman, 1927), though prismatic crystals have also been described (Aminoff, 1923).

Silicate

A composition close to the ideal formula of a serpentine mineral is indicated by the chemical analysis. The low iron content is compatible with the observed yellowish color. Magnusson (1930) states that the silicate part of the intergrowth has the composition $Mg_3Si_2O_5(OH)_4$.

The structural features of the serpentine minerals are complex (see Whittaker & Zussman, 1956; Wicks & Whittaker, 1975, for a review). The basic structure building unit in all of these structures is a slab consisting of one layer of magnesium hydroxide octahedra and one silicate sheet with six-rings of tetrahedra. In lizardite the slabs are planar, while they form rolls in chrysotile. In antigorite there are regular reversals in the position of the octahedral and the tetrahedral layers, giving each slab a wavy appearance (Kunze, 1956). One wavelength contains m tetrahedral units of length 2·55 Å, and this produces a variable lattice repeat of $a = m \times 2{\cdot}55$ Å. With each reversal within a slab, some Mg and OH is removed. The composition of antigorite is thus dependent on the lattice repeat as can be seen from the formula

$m[Mg_{3(1-1/m)}Si_2O_5(OH)_{1+3(1-2/m)}]$ (Bailey, 1984).

The observed *c*-axis length of 7·3 Å, variable *a*-axis repeat and pronounced hexagonal sublattice (a = 5·1 Å) in the a^*b^* diffraction pattern (Fig. 4) identify the silicate as an antigorite. Most antigorites have an *a*-axis repeat in the ranges $10 < m < 20$ (common) and $31 < m < 43$ (less common), see Zussman, Brindley & Comer (1957), Chapman & Zussman (1959) and Bailey (1984). Phases with $6 < m < 8$ are probably carlosturanite instead of antigorite (Mellini & Zussman, 1986). All antigorite laths in the present study belong to the category $10 < m < 20$. A single lattice repeat (m = 16) is given in Kautz (1967). As can be seen in Fig. 5, the experimental *a* repeats are clustered around the lines corresponding to integer m values. The deviation from the lines corresponding to integer m values is mostly due to experimental error. It has also been assumed that the *b* repeat is constant. Another possibility that must be taken into consideration is that m really deviates from integer values owing to the averaging effects inherent in the diffraction method. More than one lattice repeat can be present in the area of diffraction, as shown in Fig. 4.

A common phenomenon among layer silicates is disorder in the slab stacking along **c**. If two adjacent slabs are related by the vector $p \times \mathbf{b}/3$, where p = 0,1,−1 in a random fashion, it can be shown that reflections hkl, $k = 3n$ will be unaffected, while the rest of the reflections will lose intensity (Brindley, 1984). This intensity distribution is evident for the antigorite reflections in Figs. 2(*a*,*b*). The same thing was noted by Kunze (1958; see his Figs. 3 and 6) and further discussed in Kunze (1959). Since the antigorite slabs are corrugated, only translations along **b** are possible when the slabs are stacked. This stacking disorder gives streaking along **c***, which can be seen in Figs. 2 and 3. According to Kunze (1959), no streaking is observed for the reflections hkl, $k = 3n$. This does not apply here, since this type of reflection also exhibits streaking.

The antigorite laths are flattened on {001}, as is usually the case with antigorite crystals (Zussman, Brindley & Comer, 1957). What is more unusual is the extreme elongation along **b** which gives the crystals an asbestiform habit. Antigorites fibrous along the *b* axis have sometimes been given the name 'picrolite' (Mellini & Zussman, 1986).

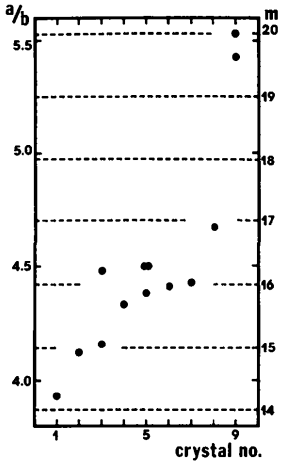

Fig. 5. Distribution of lattice-constant ratios *a*/*b* in some antigorite laths. More than one entry for a specific crystal corresponds to different parts of this crystal.

Arsenate–silicate intergrowth

It is evident from our limited data on 'asbestos–hedyphane' that the amount of antigorite present in the material is highly variable. The amount of rotational disorder along the fiber axis is considerable and it also varies from specimen to specimen. Despite this, the X-ray experiments demonstrate a preferred orientation between the arsenate and the antigorite. A combination of crystallographic and morphological data indicates that the contact plane is {001} for antigorite and a prism face {*h*,*k*,−(*h*+*k*), 0} on the hedyphane-like phase. The most common prism face on crystals with the apatite type of structure is $\{10\bar{1}0\}$ (Rahmdor & Strunz, 1978). Unit meshes of these planes are: antigorite {001}, $a = m \times 2{\cdot}55$, $b = 9{\cdot}23$ Å, $\gamma = 90°$; and arsenate $\{10\bar{1}0\}$, $a = 10{\cdot}05$, $c = 7{\cdot}31$ Å, $\beta = 90°$. The following axes are parallel: **a**(antigorite) ∥ **a**(arsenate), and **b**(antigorite) ∥ **c**(arsenate). This gives the following lattice relationships, if m is equal to 1 for simplicity: $4a$(antigorite) ≃ a(arsenate) and $4b$ (antigorite) ≃ $5c$(arsenate). This relationship was also reported by Kautz (1967). The next low-index prism face on the arsenate is $\{11\bar{2}0\}$, with an orthogonal unit mesh of $3^{1/2}a = 17{\cdot}42$, $b = 7{\cdot}31$ Å. With **b**(antigorite) ∥ **c**(arsenate) and $m = 1$ as before, the lattice coincidence becomes $7a$(antigorite) ≃ $3^{1/2}a$(arsenate).

The difference in lattice dimensions is only a few % in both cases, but the area of the coincidence meshes is large, or about 370 and 650 Å^2. Since the real cell of antigorite has been neglected, some doubt is cast on the relevance of lattice fit in the case of 'asbestos–hedyphane', especially since we have so far not been able to find a fit between the crystal structures of hedyphane and antigorite on the relevant planes.

A schematic model of rotational ordering in the intergrowth is presented in Fig. 6. It is assumed that most of the {001} laths of antigorite grow on the arsenate prisms $\{10\bar{1}0\}$. The angle between two laths is then a multiple of 60°. A lesser number of laths grow on the $\{11\bar{2}0\}$ prisms. Together with the first set of laths, the angle between two intersecting laths becomes a multiple of 30°. This model is compatible with the textural effects seen on the Weissenberg films and in the scanning electron micrographs.

This intergrowth of a flexible silicate and a brittle arsenate, found in nature, is similar to some of the man-made composite materials which have been produced in search of solids with useful properties. According to the classification of composite materials based on the connectivity of the two components (Newnham, Skinner & Cross, 1978), this mineral aggregate is best described as a 1D–1D material, because it is easy to separate the fibers from each other.

Another interesting natural composite material is bone and tooth enamel, which is an intergrowth of an apatite phase, $Ca_5P_3O_{12}(OH)$, and organic fibers (collagen). This can be compared to 'asbestos–hedyphane', which is an intergrowth of an arsenate–apatite and silicate fibers. Is it a mere coincidence that the third combination, *i.e.* asbestiform silicate plus collagen fibers, also exists? It is known that chrysotile and crocidolite fibers can cause hardening of the lung tissues in humans who are exposed to asbestos dust in the environment. This hardening is caused by collagen growth and can lead to the pulmonary disease asbestosis (Ross, 1981).

A rough description of an intergrowth of two crystal structures includes the dimensionality of the two components and the scale of the intergrowth. This scale ranges from unit-cell level to macroscopic level or, to take two specific examples: from ZnS polytypes (intergrowths of sphalerite and wurtzite structures), to a graphic granite (an intergrowth of feldspar and quartz on the cm scale). We note in passing that a dimensionality scheme, similar to that developed by Newnham *et al.* (1978) for composite materials, is a general solution to the problem of crystal-structure description and classification. A great advantage with this system is its independence of space groups and symmetry operations.

In the case of intergrowths, different degrees of order are encountered. First of all, the orientational freedom of the two building units decreases with increasing dimensionality of building units, *e.g.* there are more ways to arrange a set of blocks (0 dimensional) than ways to arrange a stack of slabs (2 dimensional). For 3-dimensional building units the restrictions are rather severe, *cf.* two interpenetrating nets. Thus, depending on the morphology of the building units, different textures are possible. The next degree of freedom concerns the relationship between the morphology of a building unit and its crystallographic axes, *e.g.* if the units are rods (1 dimensional), it is possible to have all rods elongated along the same crystallographic direction or, at the other extreme, each individual rod can have a unique non-crystallographic direction of elongation. Finally, there is, in the case of a crystallographically well defined intergrowth (epitaxy), the possibility of a lattice/structural fit. The variability observed in real intergrowths is caused by the competition of external and internal (structural) factors during the process of formation.

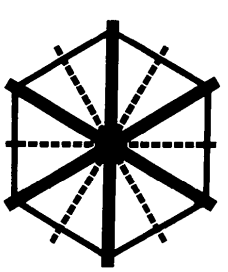

Fig. 6. Schematic model of the intergrowth seen along **c** (arsenate) or **b** (antigorite). Hexagonal arsenate crystal penetrated by antigorite laths parallel to the first hexagonal prism (thick lines). A less-common orientation of the antigorite is along the second hexagonal prism (dashed lines).

Intergrowths containing serpentine can, from a crystal chemical point of view, be divided into three groups: (i) those which show a large similarity in crystal structure and chemical composition between the two components; (ii) those with a partial correspondence in structure and chemistry; and finally (iii) those in which the two constituent parts only show little relationship with each other.

Intimate intergrowths of the different serpentine minerals clearly belong to the first group. Serpentine intergrowths were known from X-ray studies, *e.g.* Wondratschek (1957), but have during the last decade been successfully studied by transmission electron microscopy (TEM), *e.g.* by Veblen & Buseck (1979, 1981). Electron micrographs have demonstrated that the classification of serpentine as lizardite/chrysotile/antigorite is only a rough outline of the structural variations possible in this group, since the three structure types can intergrow on the nanometer scale to form structures of intermediate nature. An example is the so-called Povlen-type chrysotile ('schweizerite'), which has been shown to consist of fibers built of a polygonal arrangement of planar serpentine laths, sometimes with a chrysotile roll at the center (Cressey & Zussman, 1976). The crystal structure of carlosturanite is related to that of flat-layer serpentine by substitution of $(Si_2O_7)^{6-}$ groups along **b** in the silicate sheet by $[(OH)_6H_2O]^{6-}$, as proposed by Mellini, Ferraris & Compagnoni (1985). Coherent intergrowths of serpentine and carlosturanite were observed by TEM. Parallel intergrowths of carlosturanite, chrysotile and brucite fibers were also found (Compagnoni, Ferraris & Mellini, 1985).

Examples of oriented intergrowths of two components with partial structural and chemical similarity include serpentines plus biopyriboles (*i.e.* micas, pyroxenes and amphiboles) or certain layer silicates like talc and chlorite (Veblen & Buseck, 1979, 1981). An alternating intergrowth of slabs of phlogopite mica and serpentine has been characterized as 'eastonite' by Livi

& Veblen (1987). Another member of this group is 'nemalite', which consists of parallel fibers of brucite, $Mg(OH)_2$, and chrysotile, see Whittaker & Middleton (1979) and references cited therein. Since the outside of a chrysotile roll consists of a curved magnesium hydroxide layer, it might be expected that this layer would be parallel to the same type of layer in the brucite part of the intergrowth. But in reality this is only rarely observed!

In the last group, where the structural and chemical similarity between the components is small, several types of behavior are observed for intergrowths of chrysotile rolls and fibers of other minerals. Wondratschek (1957) identified three different crystallographic axes as the fiber axis of calcite ($CaCO_3$) from calcite–chrysotile specimens. A planar lattice fit is possible in all three cases. Magnesite–chrysotile intergrowths, on the other hand, exhibited magnesite ($MgCO_3$) with three types of crystallographic axis, offset from the fiber axis by 0·5–4°, and no likely lattice relationship between the two phases (Whittaker & Middleton, 1979). Magnetite (Fe_3O_4) fibers in chrysotile from Shabani, Zimbabwe, showed two distinct lattice directions along the fiber axis, but no lattice fit, while similar magnetite fibers from Québec, Canada, did not have a specific lattice direction along their length (Whittaker & Middleton, 1979).

The examples given above indicate that oriented intergrowth is indeed a complex phenomenon and that a structural fit between the two components becomes a less-important factor when going from the first group to the third group. 'Asbestos–hedyphane' clearly belongs to the third group of materials. Our guess is that both minerals have crystallized together in such a way that the first phase formed an anisotropic environment for the second phase during crystallization, and *vice versa*, thus enhancing a tendency for the formation of elongated crystals, present in both phases. This would account for the perfect parallelism of **b** (antigorite) and **c** (arsenate) along the fiber axis. The presence of a lattice fit between (001) antigorite and $(10\bar{1}0)$, $(11\bar{2}0)$ arsenate could possibly be the reason why the two types of crystal do not exhibit complete rotational disorder around the fiber axis. Instead a preferred orientation of the silicate occurs after every 60° (or 30°) of rotation around the fiber axis.

We thank L. Närlund for providing one of the mineral specimens and H. van Ass for the chemical analysis. This work was supported by a grant (DMR 8418083) from the National Science Foundation.

References

AMINOFF, G. (1923). *Geol. Foeren. Stockholm Foerh.* **45**, 124–143.

BAILEY, S. W. (1984). *Structures of Layer Silicates.* In *Crystal Structures of Clay Minerals and their X-ray Identification,* edited by G. W. BRINDLEY & G. BROWN, pp. 1–124. London: The Mineralogical Society.

BRINDLEY, G. W. (1984). *Order–Disorder in Clay Mineral Structures.* In *Crystal Structures of Clay Minerals and their X-ray Identification,* edited by G. W. BRINDLEY & G. BROWN, pp. 125–195. London: The Mineralogical Society.

CHAPMAN, J. A. & ZUSSMAN, J. (1959). *Acta Cryst.* **12**, 550–552.

COMPAGNONI, R., FERRARIS, G. & MELLINI, M. (1985). *Am. Mineral.* **70**, 767–772.

CRESSEY, B. A. & ZUSSMAN, J. (1976). *Can. Mineral.* **14**, 307–313.

DUNN, P. J., PETERSEN, E. U. & PEACOR, D. R. (1985). *Can. Mineral.* **23**, 251–254.

DUNN, P. J., ROUSE, R. C. & NELEN, J. A. (1985). *Geol. Foeren. Stockholm Foerh.* **107**, 325–327.

KAUTZ, K. (1967). *Contrib. Mineral. Petrol.* **14**, 224–228.

KUNZE, G. (1956). *Z. Kristallogr.* **108**, 82–107.

KUNZE, G. (1958). *Z. Kristallogr.* **110**, 282–320.

KUNZE, G. (1959). *Z. Kristallogr.* **111**, 190–212.

LIVI, K. J. T. & VEBLEN, D. R. (1987). *Am. Mineral.* **72**, 113–125.

MAGNUSSON, N. H. (1930). *Sver. Geol. Unders. Ser. Ca.* **23**, 1–111.

MELLINI, M., FERRARIS, G. & COMPAGNONI, R. (1985). *Am. Mineral.* **70**, 773–781.

MELLINI, M. & ZUSSMAN, J. (1986). *Mineral. Mag.* **50**, 675–679.

NEWNHAM, R. E., SKINNER, D. P. & CROSS, L. E. (1978). *Mater. Res. Bull.* **13**, 525–536.

PALACHE, C. & BERMAN, H. (1927). *Am. Mineral.* **12**, 180–187.

RAHMDOHR, P. & STRUNZ, H. (1978). *Klockmanns Lehrbuch der Mineralogie,* 16th ed., pp. 635–639. Stuttgart: Ferdinand Enke.

ROSS, M. (1981). *The Geological Occurrences and Health Hazards of Amphibole and Serpentine Asbestos.* In *Amphiboles and Other Hydrous Pyriboles – Mineralogy. Reviews in Mineralogy* 9A, edited by D. R. VEBLEN, pp. 279–323. Washington: Mineralogical Society of America.

ROUSE, R. C., DUNN, P. J. & PEACOR, D. R. (1984). *Am. Mineral.* **69**, 920–927.

SJÖGREN, HJ. (1891). *Geol. Foeren. Stockholm Foerh.* **13**, 781–789.

SJÖGREN, HJ. (1892). *Bull. Geol. Inst. Univ. Upsala,* **1**, 1–64.

VEBLEN, D. R. & BUSECK, P. R. (1979). *Science,* **206**, 1398–1400.

VEBLEN, D. R. & BUSECK, P. R. (1981). *Am. Mineral.* **66**, 1107–1134.

WHITTAKER, E. J. W. & MIDDLETON, A. P. (1979). *Can. Mineral.* **17**, 699–702.

WHITTAKER, E. J. W. & ZUSSMAN, J. (1956). *Mineral. Mag.* **31**, 107–126.

WICKS, F. J. & WHITTAKER, E. J. W. (1975). *Can. Mineral.* **13**, 227–243.

WICKS, F. J. & ZUSSMAN, J. (1975). *Can. Mineral.* **13**, 244–258.

WONDRATSCHEK, H. (1957). *Neues Jahrb. Mineral. Monatsh.* pp. 135–140.

ZUSSMAN, J., BRINDLEY, G. W. & COMER, J. J. (1957). *Am. Mineral.* **42**, 133–153.